Portable Indentation Plastometry for Accurate and Immediate In-ditch Material Verification

James Dean
Plastometrex

Pipeline Pigging and Integrity Management Conference

February 12-16, 2024

CLARION
TECHNICAL CONFERENCES

Organized by
Clarion Technical Conferences

https://doi.org/10.52202/072781-0085

https://doi.org/10.52202/072781-0085

Abstract

Profilometry-based Indentation Plastometry (PIP) testing is a novel approach for measuring stress-strain curves from indentation tests. It differs from scratch testing and Instrumented Indentation Testing (IIT) in several important ways which are covered in this paper. The underlying scientific methodology (an accelerated inverse finite element analysis) is also discussed. A new tool for in-ditch Material Verification that employs PIP testing is now available and in use, but to support its adoption on oil and gas transmission pipelines, the tool has recently been subjected to a period of intense validation in cooperation with several network operators, several service providers, and the PRCI. By June 2023, 125 pipes had been tested. Those test results indicated that the tool has industry-leading accuracy levels (MAPE numbers) which is expected to be of interest to pipeline integrity management teams. These assertions have been corroborated through independent analyses of the validation testing data by RSI Pipeline Solutions LLC. In addition to MAPE numbers, alternative metrics for characterizing the accuracy of this and other tools for material verification were also examined (through tests conducted on the same pipe samples). These statistical methods included Clopper-Pearson, Hanson-Koopman, a one-sided prediction interval method, and a linear regression method, with the outcome being that PIP testing is extremely well suited for fast, accurate and repeatable measurement of pipeline material properties.

The paper will cover the details of the validation testing journey, the validation test results, and the statistical analyses that were conducted.

1. Introduction

A lack of Traceable, Verifiable, and Complete (TVC) records for onshore gas transmission pipelines has driven new regulation in North America (the so-called "Mega Rule"). The data in these records, when available, are used to support safe operation of pipeline assets, often in the form of engineering critical assessments and/or maximum operating pressure calculations which often require knowledge of yield and tensile strengths. The regulation therefore mandates that these strength characteristics be determined for sections of pipe where records don't exist, and this has driven the development or enhancement of technologies for their in-situ measurement. Two such technologies (the MMT HSD tester and the Frontics IIT) are already being used following comprehensive validation studies that are publicly available from the Pipeline Research Council International (PRCI report number PR-335-173816-R01) and the Gas Technology Institute (GTI project number 22428/22429). An alternative technology for in-ditch strength measurements is currently under development at Plastometrex (PLX) – a science and technology company based in Cambridge (UK). Prior to its release (scheduled for late 2023), an equally comprehensive set of validation tests has been requested by representatives from the midstream oil and gas industry. This report covers the background to these tests, along with test outcomes and accuracy statements in the format typically requested by pipeline integrity professionals.

https://doi.org/10.52202/072781-0085

1.1. Methods for extracting stress-strain curves from indentation data

Two main conceptual approaches have been adopted for the extraction of stress-strain curves from indentation test data. The first, commonly termed the "Instrumented Indentation Technique" (IIT), involves converting load-displacement data from a spherical indentation test directly to stress-strain curves using analytical relationships. The second is "Profilometry-based Indentation Plastometry" (PIP) testing, which also utilises a spherical indenter, and includes the measurement of the surface profile after the creation of the indent coupled with inverse finite element analysis to determine the stress-strain curve.

1.1.1. Instrumented indentation technique (IIT)

This approach has been very popular [1-14] and is attractive in terms of quickly and easily obtaining the outcome, but it involves gross simplifications concerning the actual stress and strain fields under an indenter. A slight variant of the concept involves the use of neural network procedures [15-17] to relate load-displacement data to corresponding stress-strain curves – i.e. to "train" the analytical relationship, although in practice this is subject to similar limitations. In fact, it has become clear [18] that the reliability of the IIT approach is in general very poor. This largely arises from the complexity of the evolving stress and strain fields during indentation, which cannot be analytically linked to the load-displacement data in an accurate, universal way. This applies equally to neural network approaches, which also seek an empirical functional relationship of some sort.

1.1.2. Profilometry-based indentation plastometry (PIP)

The second approach is a more rigorous one, although inevitably more cumbersome. It involves [19-25] creation of the indent, measurement of the surface profile and repeated FEM simulation of the indentation test, altering the values of the parameters in a constitutive plasticity law until optimum agreement is reached between the measured and a modelled outcome.

The Plastometrex technology is focussed on the surface profile rather than the load-displacement curve as it has several advantages [26-29]. In summary, these include removal of the need for any measurements during loading (apart from the maximum attained load), elimination of uncertainties associated with machine compliance, scope for detection and analysis of (in-plane) anisotropy and an improved sensitivity of the measured outcome to the shape of the stress-strain curve.

The main conceptual distinction, however, is between direct conversion of load-displacement data to a stress-strain curve (IIT) and iterative FEM to converge on optimal values of parameters in a constitutive law. Iterative FEM simulation clearly has the potential to fully capture the nature of the evolving stress and strain fields during the test, whereas this is simply not possible with the IIT approach.

https://doi.org/10.52202/072781-0085

1.2. Experimental considerations for PIP Testing

1.2.1. Indenter geometry

Spherical indenters are used in PIP testing, the reasons for which have been discussed in detail previously [21-23, 30, 31]. A sphere is less prone to becoming damaged than sharp indenters with edges or points. It is also easier to specify and manufacture. Furthermore, there is reduced risk with spheres of encountering the computational problems that can arise with simulation of behaviour in regions of high local curvature (edges or points). These constitute powerful incentives for the use of spheres.

1.2.2. Indentation size

The size of indentation during PIP testing must be large enough such that the size of the deformed volume is representative of the bulk. For a typical polycrystalline metal, such as in pipeline steels, this translates into a requirement for a "many-grained" or representative volume to be deformed, since the plastic response of the bulk is influenced by characteristics such as grain size and shape, crystallographic texture and grain boundary structure (influencing the ease of inter-granular sliding and grain rotation).

Grain size is commonly in the range of a few microns up to a few hundred microns. Therefore, an indenter with a radius of 1 mm penetrating to a depth of around 200 microns will always test a representative volume of the metal. Figure 1 shows an example of an indent with these characteristics into a material with a grain size of 100-200 microns, confirming that the indent straddles a significant number of grains.

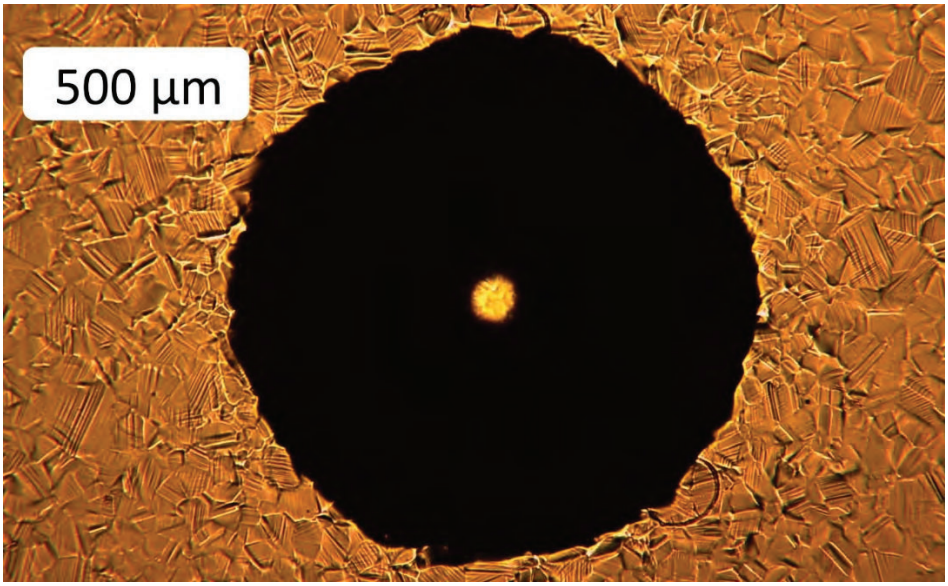

Figure 1. Optical micrograph of a residual indent following a PIP test into polycrystalline copper with an Indentation Plastometer. The indent is radially symmetric, which indicates that the material is at least isotropic in the plane normal to the indent direction. It is also evident that the indent straddles multiple grains, and that a representative volume of material has been interrogated.

https://doi.org/10.52202/072781-0085

1.2.3. Plastic strain levels

In addition to the requirement to deform a volume that is large enough to be representative of the bulk, it is important that the plastic strains being induced in the deformed region should be in an appropriate range. In most cases, interest centres on a range up to several tens of % (since these are levels that commonly occur prior to fracture of most metallic materials during tensile testing). A test in which peak strains are well below this range cannot reveal reliable information about the plasticity characteristics of interest. This is a different requirement from that of the volume (relative to the grain size). For a spherical indenter, the distribution of plastic strain beneath the indenter depends on the penetration ratio, ∂/R, with the stress and strain fields during indentation being independent of the absolute scale. The distribution of strain also depends on the plasticity characteristics of the sample, but in general it is found that a ∂/R value of about 10-20% produces a suitable plastic strain distribution [23, 32] and, therefore, enhanced confidence in the stress-strain curve at high strains.

1.2.4. Target Outcomes

Either the load-displacement plot or the residual indent profile can be used as the target outcome, but the latter offers several advantages over the former and Plastometrex technologies are largely focused on it. These advantages include the fact that no measurements need to be made during the test (apart from noting the maximum load). If, on the other hand, the load-displacement plot is being used as the target outcome (as in IIT), then (accurate) displacement measurement must be made during the test, which might well require some kind of compliance calibration. Furthermore, use of the (3-D) residual indent profile offers potential for the detection and characterization of plastic anisotropy in the sample, whereas this is not possible if the focus is on load-displacement. Finally, there is an option to measure the profile at more than one depth, which provides additional experimental data and could, for example, be useful in detecting (sharp) variations in material properties with depth. Of course, using the indent profile as the target outcome does not preclude the acquisition of load-displacement data, which might be useful for process control – for example in ensuring that the test is carried out to a particular penetration depth or applied load.

There is then the issue of how the profile is measured. There are two main approaches, one involving (very low load) contact of a stylus that is dragged across the sample and the other based on (non-contact) scanning of an optical beam of some sort. Both exhibit various characteristics that are relevant to this application, with a wider range of types being available for optical measurement. Reviews are available for both stylus [33] and optical [34] systems, and either can be used to measure indentation profiles with the required accuracy of around 1 micron.

1.2.5. Inverse finite element analysis

Detailed information about the inverse finite element model formulation including the constitutive laws used to model plasticity [35,36], the effect and likely values of interfacial friction [40-47] and convergence on the best-fit plasticity characteristics (yield stress, hardening behaviour and ultimate tensile strength (UTS)) are detailed elsewhere [29]. The outcome of this operation is a modelled residual indent profile which closely matches with that obtained during the experiment. This

https://doi.org/10.52202/072781-0085

modelled profile corresponds to a set of plasticity parameters which define the full stress-strain curve of the metal.

2. Portable PIP Testing

2.1. Requirements

The guidance (from 49CFR192.607) is not very detailed, but validation by a subject matter expert is required. Note, for example, the following from a regulatory standpoint (from the Code of Federal Regulations):

§ 192.607 Verification of Pipeline Material Properties and Attributes: Onshore steel transmission pipelines.

(a) Applicability

Operators of onshore steel transmission pipelines must document and verify material properties and attributes in accordance with this section.

(b) Documentation of material properties and attributes

Records established under this section documenting physical pipeline characteristics and attributes, including diameter, wall thickness, seam type, and grade (e.g., yield strength, ultimate tensile strength, or pressure rating for valves and flanges, etc.), must be maintained for the life of the pipeline and be traceable, verifiable, and complete. Charpy v-notch toughness values established under this section needed to meet the requirements of the ECA method at § 192.624(c)(3) or the fracture mechanics requirements at § 192.712 must be maintained for the life of the pipeline.

(c) Verification of material properties and attributes

If an operator does not have traceable, verifiable, and complete records required by paragraph (b) of this section, the operator must develop and implement procedures for conducting non-destructive or destructive tests, examinations, and assessments in order to verify the material properties of aboveground line pipe and components, and of buried line pipe and components when excavations occur at the following opportunities: anomaly direct examinations, in-situ evaluations, repairs, remediations, maintenance, and excavations that are associated with replacements or relocations of pipeline segments that are removed from service. The procedures must also provide for the following:

1. For non-destructive tests, at each test location, material properties for minimum yield strength and ultimate tensile strength must be determined at a minimum of 5 places in at least 2 circumferential quadrants of the pipe for a minimum total of 10 test readings at each pipe cylinder location.
2. For destructive tests, at each test location, a set of material properties tests for minimum yield strength and ultimate tensile strength must be conducted on each test pipe cylinder removed from each location, in accordance with API Specification 5L.
3. Tests, examinations, and assessments must be appropriate for verifying the necessary material properties and attributes.

https://doi.org/10.52202/072781-0085

4. If toughness properties are not documented, the procedures must include accepted industry methods for verifying pipe material toughness.
5. Verification of material properties and attributes for non-line pipe components must comply with paragraph (f) of this section.

(d) Special requirements for non-destructive Methods

Procedures developed in accordance with paragraph (c) of this section for verification of material properties and attributes using non-destructive methods must:

1. Use methods, tools, procedures, and techniques that have been validated by a subject matter expert based on comparison with destructive test results on material of comparable grade and vintage.
2. Conservatively account for measurement inaccuracy and uncertainty using reliable engineering tests and analyses; and
3. Use test equipment that has been properly calibrated for comparable test materials prior to usage.

2.2. Accounting for Surface-to-Centre Variations

A limitation of all indentation (and scratch-based) test techniques is that they only interrogate the near-surface regions of the materials being tested. This is fine for homogeneous materials, but there is a particular challenge presented by certain types of pipes which is most notable when they exhibit large surface-to-centre variations in their mechanical properties. This tends to occur more frequently in pipes with a high wall thickness to diameter ratio, and/or pipes that are seam welded, and (reportedly) in high-strength, low-alloy steels, although in all cases the thermomechanical processing history plays a strong role in the development of such surface-to-centre variations.

The problem this presents is that the surface-based measurements of yield and tensile strength must be comparable to tensile test results that have been conducted in accordance with the requirements of API Specification 5L. The Specification states:

1. The yield strength, ultimate tensile strength, and elongation values shall be determined on either a flattened rectangular specimen or on a round bar specimen.
2. Transverse round bar specimens are to be secured from non-flattened pipe sections.

The machining of round bar specimens from the wall of the pipe is very difficult making Option 1 above more convenient. In addition, round bar specimens do not sample the entire wall thickness. However, it is well documented that the pipe flattening process introduces a high degree of variability into the tensile test results, and no standard for the pipe flattening process currently exists. In addition, inter-lab variations between nominally identical specimens are common and even quite large, meaning "truth" data are often inconsistent and therefore unreliable. Nevertheless, technology providers like Plastometrex are required to demonstrate agreement with full thickness flattened transverse direction tensile test results and an accepted practice for doing so is to apply **empirically based adjustments** that act to align the surface-based measurements to the flattened transverse full-

https://doi.org/10.52202/072781-0085

thickness measurements through (traditionally) knowledge of metal composition, grain size, and wall thickness to pipe diameter ratios.

2.3. Previous Round Robin Trial Results

There have been two prior round-robin trials to evaluate the MMT HSD and Frontics test devices (along with other methods for establishing yield and tensile strength). The first was conducted in 2018 and published by the PRCI (contract PR-335-173816). Fifty samples were examined and tested. The second was conducted by the Gas Technology Institute, or GTI (Project Number 22428/22429) where seventy samples were examined and tested. Full details are contained within the respective reports. In the PRCI project, predictions from the MMT HSD, Frontics, and CheckMate algorithms were compared against the average of 3 flattened transverse test results, or a single longitudinal test result where necessary for compliance with API 5L. The 0.5% extension under load yield stress was used in all cases. The results are summarised in Table 1 (yield stress) and Table 2 (tensile strength).

Table 1. Yield stress results from the PRCI Round-Robin, May 2018, ×50 test samples.

Technique	MAPE (%)	% ± 10%	% ± 15%	% ± 20%	Maximum Overprediction (%)
MMT HSD Tester	7.0	78.0	92.0	98.0	13.4
Frontics IIT	7.6	71.4	87.8	93.9	34.6
CheckMate (10 kg load)	8.4	68.0	80.0	94.0	21.8

Table 2. UTS results from the PRCI Round-Robin, May 2018, ×50 test samples.

Technique	MAPE (%)	% ± 10%	% ± 15%	% ± 20%	Maximum Overprediction (%)
MMT HSD Tester	4.4	92.0	100.0	100.0	-
Frontics IIT	6.0	85.7	95.9	98.0	-
CheckMate (10 kg load)	8.1	74.0	82.0	90.0	-

Note that the lower the MAPE (mean absolute percentage error) value the better. It is also better to have values close to 100% in the percentage error ranges, and a low maximum overprediction is advantageous. In fact, over-prediction is unconservative from an integrity management and MAOP reconfirmation perspective. Under-prediction is conservative, but as most of the relevant analyses have conservatism built into them, then overly conservative results can ensue, which is also problematic.

From the PRCI report, the MMT HSD tester (marginally) outperformed the Frontics equipment and the CheckMate algorithm, having the lowest Mean Absolute Percentage Error (MAPE), the lowest Maximum Overprediction (for yield stress data), and the highest proportion of yield and UTS data

https://doi.org/10.52202/072781-0085

that lie within well-defined error bands. One caveat noted in the PRCI report is that the measured strength data derived from destructive laboratory testing should not be considered consistent and exactly reproducible. This followed the detection of "significant variability" between replicate transverse tensile test specimens, with an average normalised variation of 5.7%, with 18% of the (×50) specimen set having an average normalised variation greater than 10%. The origin of this variation was deemed to be influenced by several things, including:

1. The details of the laboratory tensile test procedure used to generate the data used as the benchmark for comparison.
2. The type of destructive tensile test specimen that is used (orientation and shape) for the benchmark testing vs the specimen type that was used by the service provider to develop the algorithm(s) relating in-situ data to tensile properties.
3. The spatial separation between in situ test location and destructive test specimen origin, due to the non-homogeneous nature of the material.
4. Possible differences between the definition of "yield strength" used in tensile tests as comparison benchmarks and the yield stress definition used to develop correlations between in-situ measurements and tensile test results.

One of the primary objectives of the PRCI report was to "investigate and quantify the capabilities and limitations of different NDE technologies that are identified as feasible for the characterisation of material properties…". This was accomplished in part though publication of the data in Tables 1 and 2. The primary objective of the GTI project was a little different, as it was commissioned to develop correlative models for predicting bulk properties from surface-based measurements. 70 samples were tested in that project, and were chosen to adequately cover the variety of pipes that are typically encountered by industry in the field, including:

1. Installation years from 1930 to 2004 with over 60% pre-code pipelines.
2. Diameters from 4 to 30 inches.
3. Grades from A to X52.
4. All steel types: rimmed/capped, semi-killed, and fully killed.
5. All key long seam types: ERW (electrical resistance weld), SAW (submerged arc weld), Seamless, and Spiral.
6. Wall thickness over a wide range: 0.156 to 0.460 inches.
7. Chemistry grade variety, e.g.: 1008, 1010, 1015, 1016, 1021, 1022, 1023, 1025, 1026, 1030, 1522, 1525, and vanadium and niobium High-Strength Low-Alloy (HSLA) grades.
8. ASTM grain size (log scale) range spanning: 7.0 to 13.0.

Interestingly, the study concluded that the properties of the normalised/annealed seamless pipes were mostly uniform and (sic) homogeneous through the wall. For seamed pipelines, however, there was significant inhomogeneity through the wall (and, therefore, detectable differences between surface measurements and full wall thickness data). The inhomogeneities were attributed to:

https://doi.org/10.52202/072781-0085

1. Cold work and forming stress from pipe manufacturing (without post-production normalising/annealing as in seamless pipe).
2. Chemical segregation from primary steel production (e.g., rimmed/capped centreline carbon segregation).
3. HSLA steel grain refinement especially near the outer surfaces of the pipe wall.
4. Other thermomechanical factors.

Another important difference between the PRCI and GTI reports is that, in the PRCI report, yield stress and UTS measurements were compared (primarily) against transverse flattened full wall thickness data (at 0.5% elongation under load for yield stress) as per the API 5L specification. In the GTI report, yield stress and UTS measurements were compared against "**mini**", full wall thickness **longitudinal** test results (at 0.2% offset for the Frontics equipment and at 0.5% elongation under load for the MMT HSD equipment for yield stress comparisons). This is an important distinction, because the mini, longitudinal tensile test results have been found in a previous GTI test report (GTI Project Number 20568, 2011) to have an average yield stress value that is 8.5% lower than corresponding full-size specimens tested in accordance with API 5L. When considering the complications already arising from surface-to-centre variations, as well as inter- and intra-lab variability of tensile test results, this could be considered an unfortunate complication.

A further noteworthy point from the GTI report is that several **models for adjusting surface properties to full wall properties** were tested. These included linear regression models, ordinary least squares models, Bayesian regression models, artificial neural networks, and historical empirical models. Of all the models tested, a modified version of an ordinary least squares method was the most successful model for aligning surface data with full wall data for both the MMT HSD **and** the Frontics devices.

The GTI report concluded that the best-case ordinary least squares model, when coupled with the Frontics surface data, achieved the highest performance out of the tools that were tested. The corresponding best-case model for the MMT HSD equipment exhibited a non-conservative bias on the yield stress (an over-prediction), particularly at higher yield stresses, although the calculations conducted by the GTI have been publicly contested by MMT[48]. On that basis, and until publicly resolved, the results from the GTI report have been omitted from this one.

https://doi.org/10.52202/072781-0085

3. Validation of the portable tool from Plastometrex

3.1. Project Partners

Table 3 details the organisations that supplied pipes, pipe coupons, and corresponding tensile test data to support the validation project.

Table 3. Organizations that contributed material in the form of full circumference pipes and/or pipe coupons to support the validation testing project.

Company	Pipe Coupons	Full Pipe	Tensile Test Data
SIA	Y	N	Y
Rosen	Y	Y	Y
PG&E	Y	N	Y
Plastometrex	N	Y	Y
PRCI	Y	Y	Y
Undisclosed	N	Y	Y

Table 4. Yield stress and UTS values obtained by Plastometrex on the same pipe samples when tested with both benchtop and portable systems showing good consistency across the two devices.

Plastometrex Pipe ID	YS/UTS (ksi)	Benchtop	Portable	Absolute Difference (%)	Notes
IIT36	YS	48.3	45.9	5	Seamless
	UTS	80.0	72.7	9	
IIT42	YS	64.9	65.7	1	ERW
	UTS	81.3	77.1	5	
PIP-20	YS	48.2	48.2	0	Seamless (Grade B)
	UTS	73.6	75.8	3	
PIP-25	YS	46.2	51.7	12	ERW (Grade B)
	UTS	73.0	70.4	4	
PIP-27	YS	39.9	40.6	2	Seamless
	UTS	71.1	70.4	1	

3.2. Test samples and apparatus

125 samples were collected and tested (as of 06/06/2023), including 40 of those that were tested (and were still available for testing) from the 2018 PRCI round-robin project, and 15 that were tested completely blind. The indentation tests conducted by Plastometrex utilised either the portable testing system (where full circumference pipe sections were available), or the benchtop system (where only small pipe coupons were available). Note that, where the Benchtop system was used, it was only used to create the indent; the optical scanning procedures were carried out with the portable scanning device. In any case, tests at the Plastometrex laboratory in Cambridge have previously confirmed (see Table 4) that there is good consistency between the two test devices (which is unsurprising given both

https://doi.org/10.52202/072781-0085

devices employ the same underlying scientific methodology). The maximum observed difference was 12%, with an average difference of 4%. Using the benchtop device to support the validation study was therefore deemed acceptable in those instances where it was the only realistic option for doing so.

3.3. Sample Preparation

Pipe samples that were supplied in coupon form were first mounted in Bakelite. They were then ground with silicon carbide grinding paper (80 grit, 120 grit, 240 grit, 400 grit, 800 grit, and 1200 grit, generating typical surface roughness values of ~750 nm). Full circumference pipes, for which the portable testing system was used, were prepared in a slightly different way. For example, if the pipe was coated, then the coating was first removed using a putty knife and, where necessary, a wire brush. If the pipe was corroded (found mainly on the un-coated pipes) then this was removed using an angle grinder with an abrasive flap wheel. In both cases (coated or uncoated), once the steel was exposed the surface was ground with a power file (80 grit, 160 grit, 320 grit, and 800 grit, generating typical surface roughness values of sub 1 μm). It should be noted that both surface roughness values quoted are within the accepted limit for PIP testing.

3.4. Indentation test conditions

5 repeat indents were performed on 114 of the 125 pipe samples that were tested. 3 repeat indents were performed on 11 samples, and only 2 indents were performed on 1 of the samples (due to size constraints). In each case, the first indent was performed under displacement control until a depth of ~180 μm had been reached. The peak load required to reach that depth was recorded, and all subsequent indents were performed in load control to ensure that the peak attained load for each test was directly equivalent. The displacement of the indenter head was monitored with a single LVDT (benchtop system) or a twin set of LVDTs (portable system) with a resolution of ~±1 μm. In all cases the load and displacement were monitored continuously throughout the test, although it is important to note that only the peak applied load is needed for calculation of stress-strain curves from the indentation test outcomes.

3.5. Example test data

The primary outcome of importance during a PIP test is the residual profile shape. This is the shape of the indent after the indenter has been removed and after the recovery of any stored elastic strain. In all cases, and regardless of whether the benchtop system or the portable system had been used, the residual profile shapes were measured using an optical interferometer with a vertical resolution of around 1 μm. A typical scan is shown as a 3-D contour plot inset in **Figure 2**(a), which also includes the 2-D radially symmetric profile. This 2-D profile data was processed leading to the PIP-derived stress-strain curve in **Figure 2**(b). Also included in **Figure 2**(b) is the (superimposed) stress-strain curve

https://doi.org/10.52202/072781-0085

that was measured from conventional tensile testing, showing an excellent level of agreement, even before the application of an empirical adjustment, see Section 4.2.

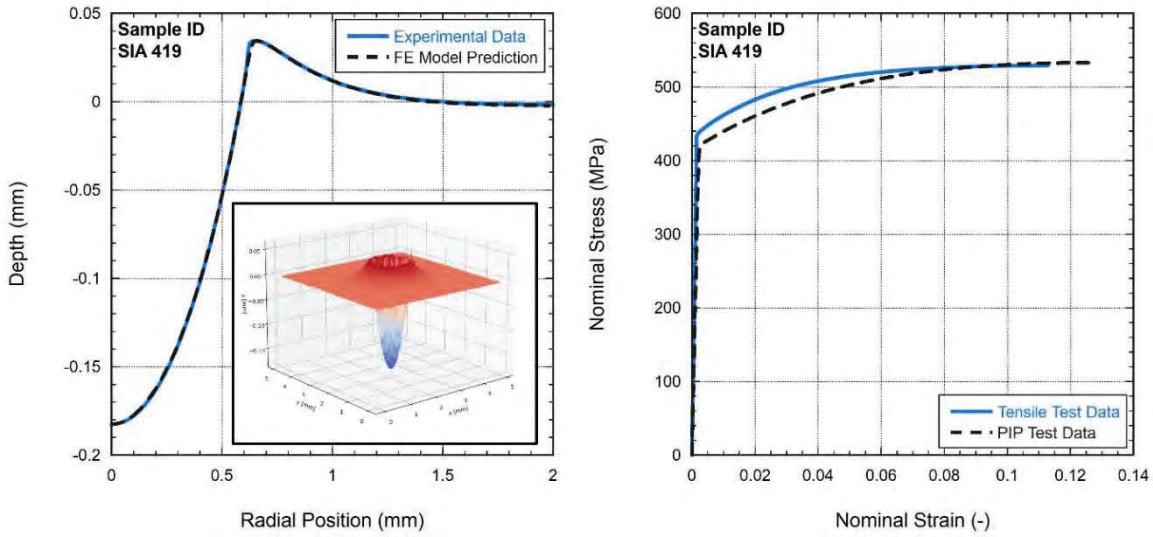

Figure 2. Measured and modelled residual profile shapes are shown in (a) in 2-D average line scan form, and (inset) in full 3-D form (measured indent only), alongside (b) the corresponding (inferred) PIP stress-strain curve, superimposed on the stress-strain curve that was obtained on the same material but from a conventional tensile test.

4. Test Results

4.1. Surface based data

The surface-based PIP test data were compared with tensile full wall thickness data for each of the samples tested. In all cases, the 0.5% elongation under load yield stress was compared. Full wall tensile data were either already available to the project (supplied by validation project partners) or measured by Plastometrex technicians in the laboratories at Cambridge in compliance with API 5L tensile testing standards. The results of these comparisons can be seen in Figure 3 in the form of unity plots for yield stress and tensile strength The following are observed:

- The surface-based PIP test yield stress tends, on average, to be lower than the flattened, transverse, full thickness tensile test result.
- The yield stress MAPE is 8.93 (across the 125 samples that were tested, noting of course that the MAPE number changes each time a new data pair are added)
- The surface-based PIP test tensile strength tends, on average, to be higher than the flattened, transverse, full thickness tensile test result
- The tensile strength MAPE is 7.71 (across the 125 samples that were tested, noting of course that the MAPE number changes each time a new data pair are added).

https://doi.org/10.52202/072781-0085

- The differences are reasonably systematic in both cases, implying a common origin for the observed differences between the surface-based measurements and the full wall thickness measurements.

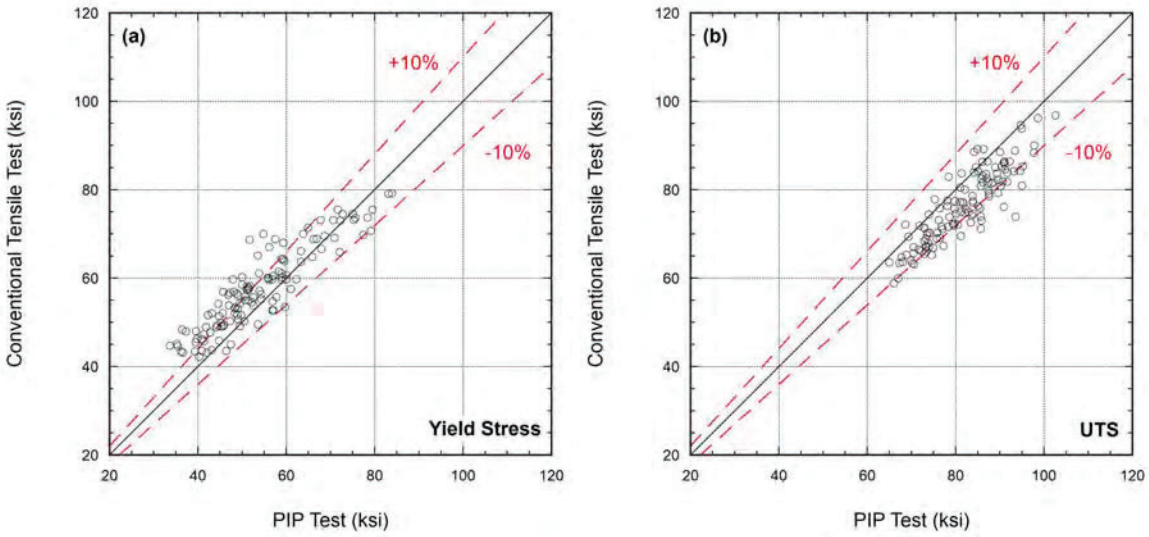

Figure 3. Unity plots for (a) yield stress and (b) tensile strength, for the validation data in their unadjusted form (surface-based data), along with ±10% error bounds.

4.2. Empirical Adjustment

The differences between the surface-based measurements and the full wall thickness measurements (**Figure 3**) were anticipated, and the midstream oil and gas industry has become accustomed to the application of "empirical correction factors" to better align the level of agreement between the two types of tests i.e. surface based tests (either indentation or scratch) and full wall tensile tests. These "corrections" often take the form of multi-parameter regression analyses or "machine learning" algorithms that combine the surface measured data with attributes such as metal composition, grain size, and pipe geometry. In fact, the machine learning algorithm that converts surface data to equivalent full wall data that is used by the MMT HSD requires no fewer than 8 model inputs [48]. The view at Plastometrex is that this is rather cumbersome, while the procedures are often unclear, and it is apparent that the adoption of such methods has been an important contributory factor in the dispute between the GTI and MMT [48]. It is also the view of Plastometrex that the terminology being used should be changed from "correction" to "adjustment", to reflect the fact that the measured surface data are in fact "correct", albeit "different" from full wall test data. This is simply a reflection of the near surface regions having different properties to the mid-wall region, and for reasons that are broadly understood.

In **Error! Reference source not found.**, the surface-based measurements that were presented in **Figure 3** have been "adjusted" so that they better correspond to the full wall tensile data. The adjustment equations that have been developed by Plastometrex and applied to the surface-based

https://doi.org/10.52202/072781-0085

data are not disclosed in this report as they are considered proprietary. However, it should be noted that the equations do not rely on knowledge of the metal composition, the metal microstructure, nor the pipe geometry. The equations developed by Plastometrex do have a dependence on the hardening (plasticity) characteristics of the metal (which are of course measured during the test), which ensures a sound physical (metallurgical) basis for the adjustment. An important point to note here is that the adjustment equations have been derived from the validation dataset in its current form (comprising these 125 samples). As the validation dataset continues to grow, it is possible that the derived constants (or even the form of the equations containing those constants) might also change, with the motivation for any such changes being a detectable increase in the accuracy of the post-adjustment data (namely a reduction in the post adjustment MAPE numbers).

Importantly, the Plastometrex adjustment can be applied instantly in the ditch, with no delay to the emergence of final and definitive stress-strain curves and metal strength data. The value of this is clear; it allows decisions to be made in real-time, problems to be addressed immediately, and the dig-site to be closed (and to remain closed) once the tests are completed.

4.3. Adjusted dataset (flattened, full wall equivalent data)

Following the adjustment:

- The PIP test yield stress MAPE reduces to 5.52.
- The PIP test UTS MAPE reduces to 3.46

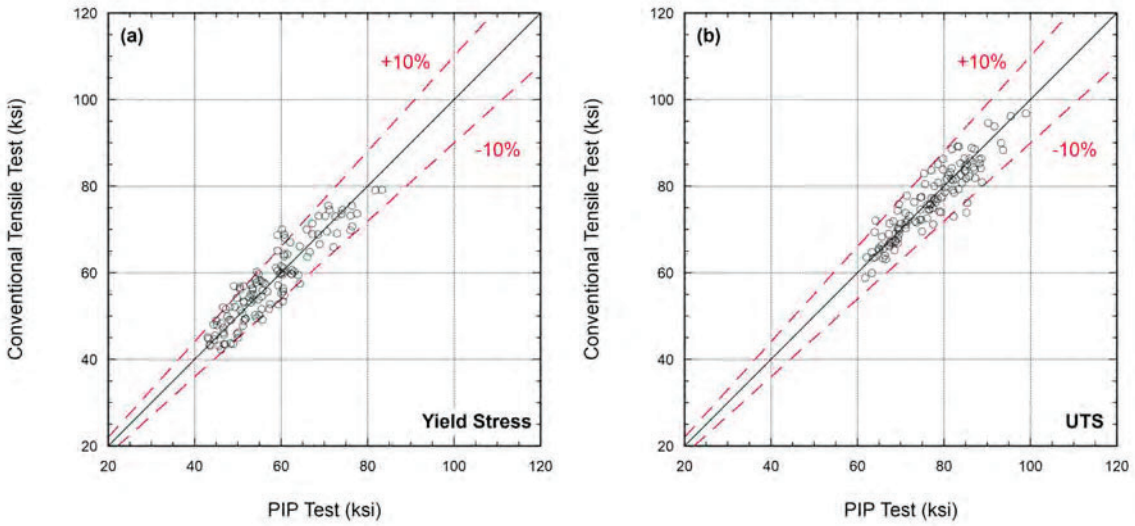

Figure 4. Unity plots for (a) yield stress and (b) tensile strength, for the validation data in their adjusted form, along with ±10% error bounds.

https://doi.org/10.52202/072781-0085

4.4. Comparisons with competing technologies and the Plastometrex accuracy statement

A summary of the test results is compiled in Table 5 and Table 6. The metrics that are shown and compared are the primary metrics that were used for comparative purposes in the PRCI report of 2018. There are two rows of Plastometrex data; one row contains the metrics obtained when using the complete 125-sample dataset; the other row contains the metrics obtained when using the (×40) PRCI samples that were still available for testing, thus permitting a (more) direct comparison to the performance of the MMT HSD and Frontics devices in 2018. There are also two rows of MMT HSD data; these are compiled from (1) the data available from the 2018 PRCI report on 50 samples, and (2) data that was later published [49] by MMT containing 167 data points[1].

The data show that the Plastometrex tool is the best performing device, with the lowest MAPE numbers for both yield stress and tensile strength, and higher proportions of test results lying within the ±10% error range. Nevertheless, it is important to recognise that the differences between the Plastometrex and MMT tools **are not substantial**, and probably represent values that are close to the limit of what is technically possible given the inherent variability in the respective tools, the inherent variability in the tensile test results, and the inherent (short and long range) variability in the properties of pipes. In contrast, and in comparisons of the PRCI testing data only, the Frontics tool is clearly inferior.

Table 5. Comparison between the performance for yield strength of the Plastometrex, MMT, and Frontics testing tools, using the primary metrics from the PRCI report of 2018 as the basis on which to compare the tools.

Organisation	Data Reference	Number of Samples	MAPE (%)	Maximum Overprediction (%)	% ± 10%	% ± 15%	% ± 20%
Plastometrex	N/A	40 (PRCI)	5.16	13.3	87.5	100.0	100.0
Plastometrex	N/A	125	5.52	13.3	86.2	100.0	100.0
MMT	MMT Report , 2020	144	5.55	15.5	85.4	95.1	100.0
MMT	PRCI Report, 2018	50	7.00	13.4	78.0	92.0	98.0
Frontics	PRCI Report, 2018	50	7.6	34.6	71.4	87.8	93.9

[1] These data pairs were obtained from the MMT publication by using the graph digitisation tool available at WebPlotDigitizer - Extract data from plots, images, and maps (automeris.io). The tool was only able to identify 144 unique data pairs. The remaining 23 are presumed to be obscured by existing datapoints. Recovery of these points *will* modify the MMT HSD MAPE number and, potentially, the order of results in Table 6.

https://doi.org/10.52202/072781-0085

Table 6. Comparison between the performance for UTS of the Plastometrex, MMT, and Frontics testing tools, using the primary metrics from the PRCI report of 2018 as the basis on which to compare the tools.

Organisation	Data Reference	Number of Samples	MAPE (%)	% ± 10%	% ± 15%	% ± 20%
Plastometrex	N/A	125	3.45	96.3	99.2	100.0
Plastometrex	N/A	40 (PRCI)	3.66	97.5	100.0	100.0
MMT	MMT Report , 2020	144	3.84	95.8	100.0	100.0
MMT	PRCI Report, 2018	50	4.40	92.0	100.0	100.0
Frontics	PRCI Report, 2018	50	6.00	85.7	95.9	98.0

4.5. Statistical analyses of tool accuracy levels

4.5.1. Overview

According to the Code of Federal Regulations (49CFR192.607), procedures developed for verification of material properties and attributes using non-destructive methods must "Conservatively account for measurement inaccuracy and uncertainty using reliable engineering tests and analyses". However, and as previously pointed out by MMT [50], there is no specific guidance about what measure of uncertainty should be used. The rule is therefore open to interpretation, and it is anecdotally evident that different statistical approaches are being adopted by different technology providers, different service providers, and different owner/operators. The scope for confusion is therefore high, as is the incentive to use more favourable statistical methods, so in due course the industry may best be served by adopting a common statistical framework in which the validation data pairs from technology providers are available for independent public scrutiny. The Plastometrex data are available from the Plastometrex website and have been subjected to four statistical treatments below. The first of these is based on the statistical approach adopted by the Pacific Gas and Electric Company, PG&E (which forms one part of a much wider probabilistic strategy for grade verification). The second is an approach adopted by an undisclosed network operator, which is a derivative of the method laid out in API 1163 for the qualification of in-line inspection systems, the third is an approach that appears to be favoured (and has been published) by MMT, and the fourth is the method adopted by Structural Integrity Associates.

4.5.2. The linear regression method (as adopted by PG&E)

The method adopted by PG&E is outlined fully elsewhere [51]. It is designed to handle uncertainty that arises from systematic effects (those that remain constant during repeated measurements) and

https://doi.org/10.52202/072781-0085

random effects (those that vary randomly between measurements). The systematic errors are accounted for by applying a least squares regression through the data points on a unity plot (see Fig.7 for an example). Following the regression analysis, the scatter in the data is quantified using a prediction interval which accounts for the random uncertainty. The outcome of this approach is that, when a non-destructive test is conducted, the measured yield and tensile strengths can be equated to a corresponding mean tensile test estimate with a corresponding uncertainty level (expressed in ksi), at a specified confidence. It is noted that, rather than choosing a particular confidence level, PG&E's approach incorporates the entire quantified distribution into additional downstream probabilistic analyses to verify grade[52, 53].

As an example, consider **Figure 5**(a) which plots tensile data against PIP test data for yield stress measurements. The solid diagonal line is the regression line – note that it is offset slightly from the unity line. It therefore depicts the systematic variation between tensile tests and PIP tests. The dashed diagonal lines are the upper and lower limits of the 80% prediction interval, where the prediction interval captures the range in which an equivalent tensile test data point is expected to lie (with some specified probability – in this case 80%) for any non-destructively measured value of the yield stress. To further clarify, if the non-destructive PIP test value for yield stress was 60 ksi, then there is an 80% probability that the (equivalent) tensile test value would lie between 55 ksi and 64.8 ksi.
The algebra can be found separately [51], but it includes an important intermediate step in which the "standard error" of the predicted value is calculated, allowing the width of the prediction interval to be found. These standard errors are plotted in **Figure 6** for the 125-sample dataset from Plastometrex, and the 144-sample dataset from MMT. The data show that the respective tools have equivalent performance on yield stress, but that the Plastometrex tool is more accurate on tensile strength (lower standard error = more accurate).

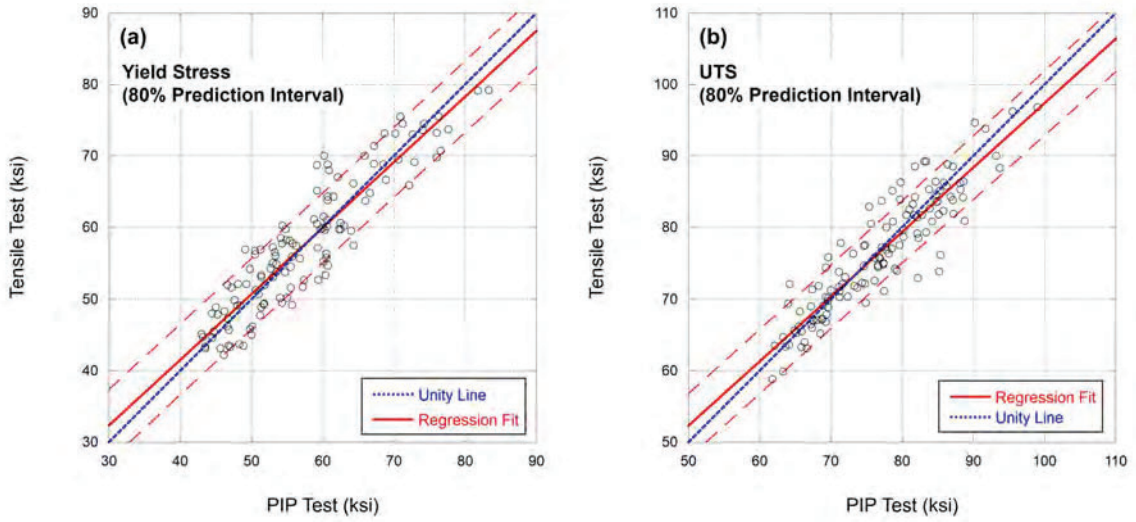

Figure 5. Unity plots for (a) yield stress and (b) UTS showing the upper and lower limits of the 80% prediction interval (dotted lines), as calculated using the method set out elsewhere [51], as well as the regression fit and the unity line.

https://doi.org/10.52202/072781-0085

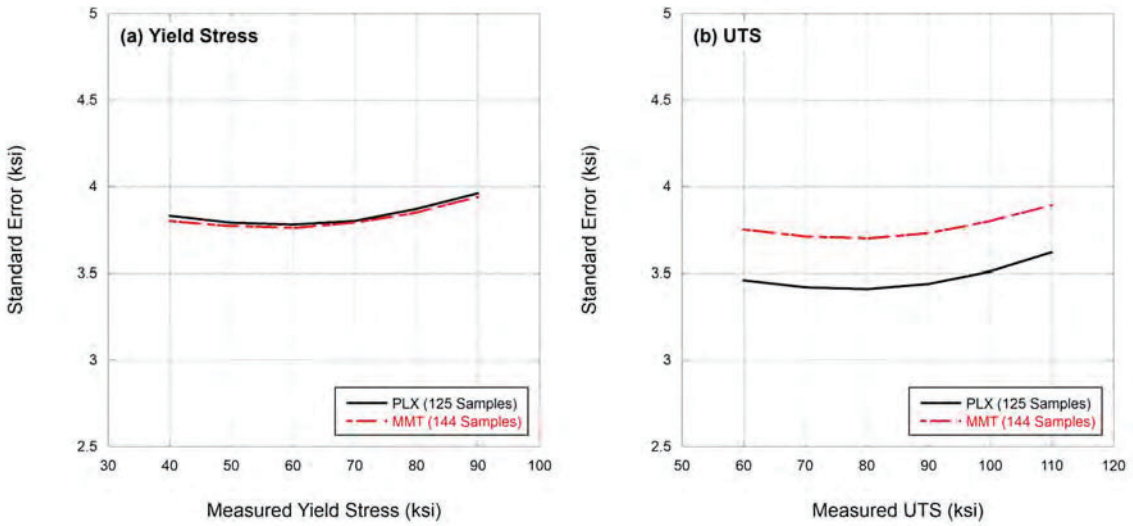

Figure 6. Calculated "standard error" (which is the terminology used in the previously cited report [51]) as a function of (a) yield stress and (b) UTS for the Plastometrex dataset (125 samples) and the MMT dataset (144 samples).

4.5.3. The Clopper-Pearson Method (as adopted by an undisclosed network operator)

This statistical method is a derivative of the method that is described in API 1163 for the qualification of in-line inspection systems. The key steps are:

1. The tool provider (i.e., Plastometrex) specifies a "tolerance" for the tool. This is a value, in ksi, that the tool provider is prepared to "rate" their tool to. For example, if the tool provider rates their tool to 10 ksi, then the tool is committed to measuring a value for the yield stress or tensile strength that is no more than 10 ksi greater than the value that would be measured from a conventional tensile test. This commitment, however, is "non-binding", and is in fact associated with a probability.
2. To calculate the probability that any tool-measured datapoint falls below the stated tolerance, there are two intermediate steps:
    a. Compute what percentage of the validation dataset falls below the stated tolerance using the simple inequality: Tool Measurement – Tensile Test Measurement < Tolerance
    b. Use the data from (a) to compute a confidence interval for the true value of this proportion using the Clopper-Pearson method.
3. Assess whether the lower limit of the calculated confidence interval is greater than 0.8 (80%). If it is, then the tool can be said to be compliant with its stated tolerance.

What this means is that 80% of the time, the true proportion of data which falls within tolerance will be inside the confidence interval produced.

Using this approach, and the 125-sample dataset, the Plastometrex tool tolerance can be set at 4.2 ksi for yield stress and 3.4 ksi for UTS (as of June 2023). Equivalent calculations on the 144-sample

https://doi.org/10.52202/072781-0085

dataset from the MMT HSD puts their tool tolerance at 3.4 ksi for both yield stress and UTS. However, it is important to note that as sample sizes get bigger, confidence intervals get narrower, so stipulating that the lower limit needs to be greater than 80% is perhaps a little peculiar, because as the confidence interval naturally narrows (with more data), the approach becomes ever more likely to produce a lower bound that exceeds the 80% requirement. The outcome is that **the tool tolerance inevitably reduces as the sample set increases**.

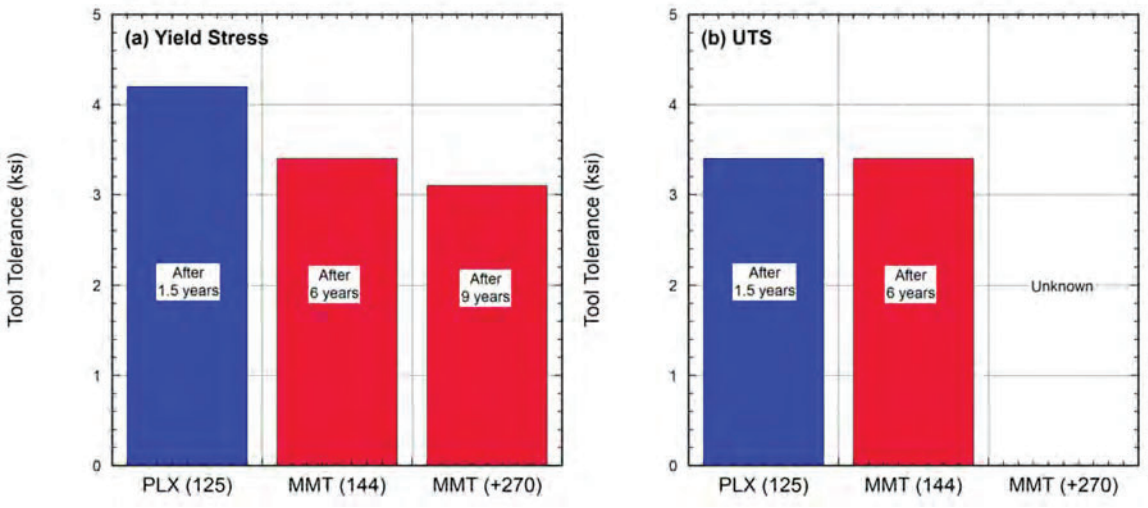

Figure 7. Comparison of the Plastometrex and MMT tool tolerance levels, as calculated using the Clopper-Pearson statistical method, and as a function of sample set size and the time taken (years of technical development) to reach that level for (a) yield stress and (b) tensile strength (UTS).

For example, the undisclosed network operator has approved the use of the MMT device on their network at a stated tool tolerance of 3.1 ksi, which is lower than the 3.4 ksi calculated on the 144-sample dataset, but MMT has recently reported[54] that its sample dataset as of February 2023 is actually greater than 270 following the recent completion of two Joint Industry Projects (although no published dataset of this size can be found online). Regrettably, with this statistical method, it is difficult to know whether the decreasing tool tolerance can be attributed to a genuine improvement in the MMT HSD tool accuracy, or whether it is just the inevitable consequence of having a larger test dataset.

4.5.4. The Hanson-Koopman method (as adopted by MMT)

The method adopted by MMT[49] bears some resemblance to the method that is used by PG&E, although this method makes no assumption about the distribution of the difference between the tensile measurement and the tool measurement, and it employs confidence intervals rather than prediction intervals.

Nevertheless, the adopted method is used to compute a measure of the uncertainty of the tool (in ksi). This describes how different a tool measurement is likely to be when compared to the equivalent tensile test measurement. Once more, the level of tool uncertainty is not fixed, but changes in

https://doi.org/10.52202/072781-0085

accordance with an assigned probability. The Hanson and Koopmans 1964 method with **50% confidence** and 80% certainty is used by MMT[50].

The 125-sample dataset from Plastometrex has been subjected to this treatment. The results are contained in **Figure 8**(a) for yield stress and **Figure 8**(b) for tensile strength. Also included are the published results[49] from MMT for comparison.

In **Figure 8**(a), we can see that at 50% confidence and 80% certainty, the tolerance for the MMT tool measured yield stress is 3 ksi. This means that, when using the tool, 50% of the time we would expect 80% of the tool measured yield stresses to be no more than 3 ksi greater than what would have been measured in a conventional tensile test. Similarly, and only 50% of the time, we would expect 95% of the tool measured yield stresses to be no more than 5.9 ksi greater than what would have been measured in a conventional tensile test.

The data show that the one-sided prediction intervals are similar, with Plastometrex outperforming MMT on UTS, and MMT slightly outperforming Plastometrex on yield stress. However, the value of this approach is significantly undermined when used at only 50% confidence, since this means that 50% of the time, the confidence interval generated will not contain the true value. In the interests of public safety, the rationale for this decision is potentially questionable (accepting that the ultimate decision on which statistical method to adopt and approve lies solely with the integrity management teams at the owner/operator companies). Equivalent plots are therefore also shown at 80% (**Figure 9**) and 95% (**Figure 10**) confidence, which are much more conventional values for analyses of this type, not least when the safety of assets and people is at risk.

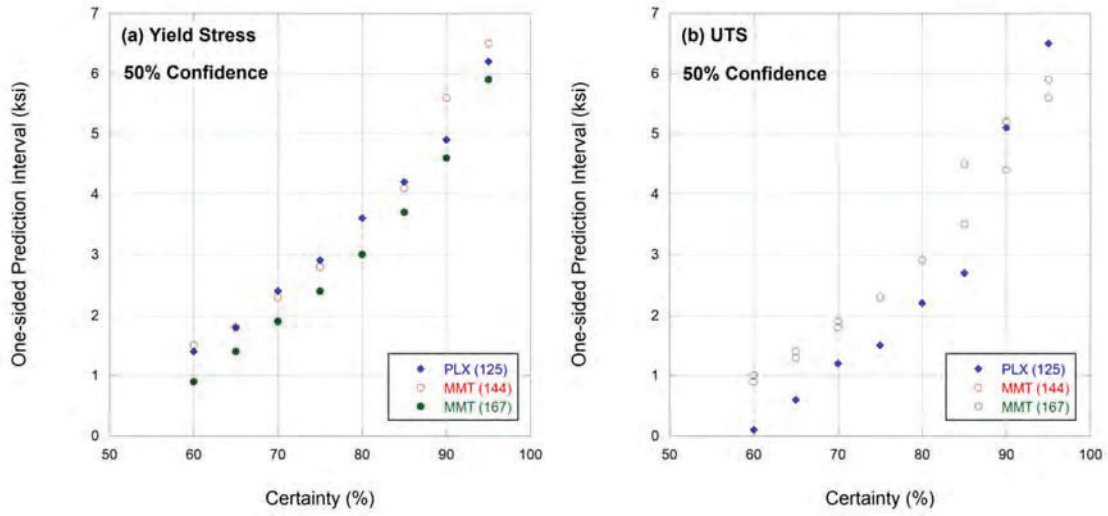

Figure 8. Calculated one-sided prediction intervals for different certainties at 50% confidence, for (a) yield stress, and (b) tensile strength (UTS).

https://doi.org/10.52202/072781-0085

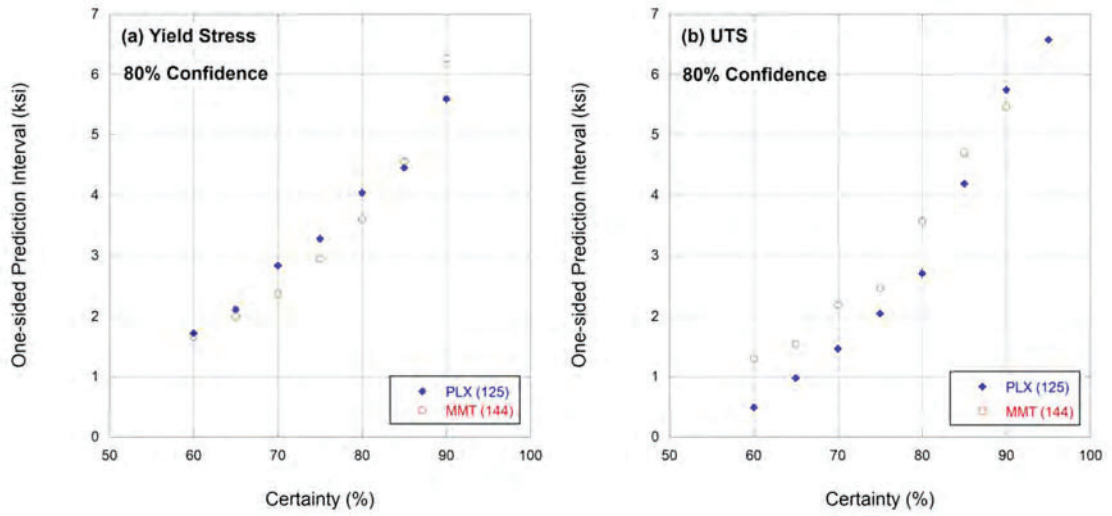

Figure 9. Calculated one-sided prediction intervals for different certainties at 80% confidence, for (a) yield stress, and (b) tensile strength (UTS).

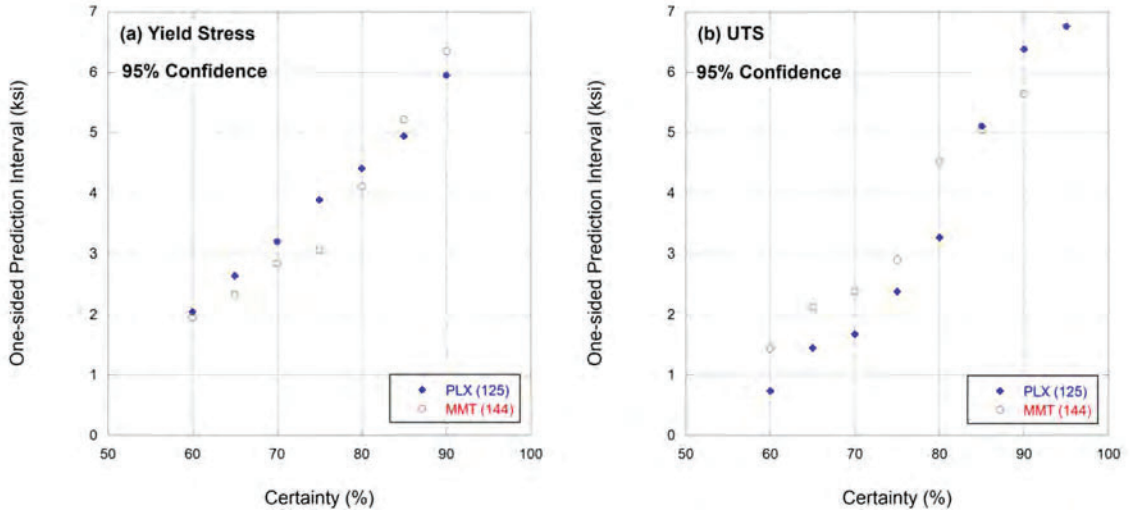

Figure 10. Calculated one-sided prediction intervals for different certainties at 95% confidence, for (a) yield stress, and (b) tensile strength (UTS).

4.5.5. The "PIP v Tensile" Prediction Interval Method (as adopted by Structural Integrity Associates)

The method adopted by Structural Integrity Associates (SIA) is similar to the method adopted by PG&E. Both methods assume normally distributed error. The steps are simple:

1. Compute the difference between the PIP tests (or scratch tests) and the tensile test data. Find the mean and standard deviation.
2. Exclude any datapoints which have error more than three standard deviations from the mean (and proceed with this "trimmed" dataset).

https://doi.org/10.52202/072781-0085

3. Build a model of the trimmed data in the form of:
   → Tensile Value = β0 + PIP Value + Error
4. Calculate a prediction interval for the error when predicting a tensile test value from a PIP test (or scratch test) value.

The outcome of applying this method to the Plastometrex and MMT HSD validation datasets is shown in **Figure 11**, which plots the one-sided prediction interval as a function of confidence level. The data show that there is little difference in performance between the Plastometrex and MMT HSD tools when adopting this method.

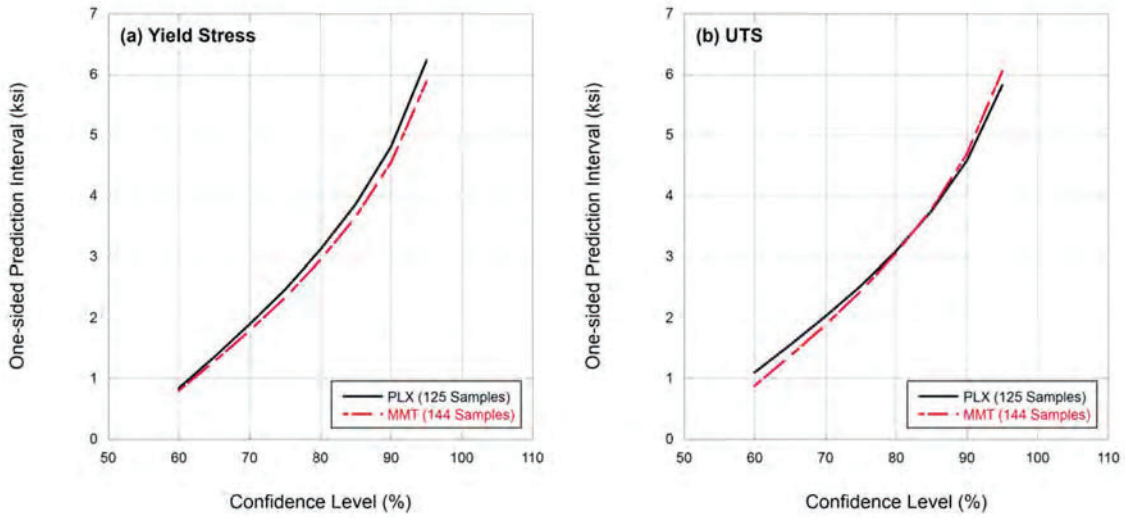

Figure 11. Calculated one-sided prections intervals as a function of confidence level for (a) yield stress, and (b) tensile strength (UTS).

https://doi.org/10.52202/072781-0085

5. Conclusions

A new tool for in-ditch testing (material verification) of oil and gas transmission pipelines has recently come to market. The tool employs an already-proven scientific methodology – Profilometry based Indentation Plastometry (PIP) – which was developed by former University of Cambridge scientists. It is an indentation-based test technology.

Prior to its deployment, the tool (and the underlying scientific method) has been subjected to a comprehensive set of validation tests. These tests have been conducted on a wide range of pipe grade, pipe diameter, wall thickness, and seam type. The tests were conducted in collaboration with PG&E, an undisclosed network operator, Structural Integrity Associates, ROSEN, and the PRCI. Test data and any subsequent analyses have been independently scrutinised by Bill Amend and Joel Anderson of RSI Pipeline Solutions.

The following conclusions have emerged:

- The Plastometrex tool has comparable accuracy to the MMT tool, and any differences (in favour of either tool) tend only to be marginal. This is true for yield strength, tensile strength, and the metric (or statistical method) employed to assess the accuracy levels.
- The Frontics tool appears to be inferior, but this assessment is based only on the Frontics data that are available from the 2018 PRCI report.
- The Plastometrex tool has a MAPE number for yield stress of 5.5.
- The Plastometrex tool has a MAPE number for tensile strength (UTS) of 3.6.
- The validation dataset is available online at www.plastometrex.com meaning it is available for public scrutiny and for others to apply their preferred statistical treatment.

References

1. B. X. Xu, X. Chen, *Determining engineering stress-strain curve directly from the load-depth curve of spherical indentation test*, J. Mater. Res., 25, **2010** 2297 https://doi.org/10.1557/jmr.2010.0310.
2. R. O. Oviasuyi, R. J. Klassen, *Deducing the stress-strain response of anisotropic Zr-2.5%Nb pressure tubing by spherical indentation testing*, J. Nucl. Mats., 432, **2013** 28 https://doi.org/10.1016/j.jnucmat.2012.07.037.
3. C. Yu, Y. H. Feng, R. Yang, G. J. Peng, Z. K. Lu, T. H. Zhang, *An integrated method to determine elastic-plastic parameters by instrumented spherical indentation*, J. Mater. Res., 29, **2014** 1095 https://doi.org/10.1557/jmr.2014.78.
4. Z. Song, K. Komvopoulos, *An elastic-plastic analysis of spherical indentation: Constitutive equations for single-indentation unloading and development of plasticity due to repeated indentation*, Mechanics of Materials, 76, **2014** 93 https://doi.org/10.1016/j.mechmat.2014.05.005.
5. S. Pathak, S. R. Kalidindi, *Spherical nanoindentation stress-strain curves*, Mat. Sci. & Eng. R, 91, **2015** 1 https://doi.org/10.1016/j.mser.2015.02.001.

https://doi.org/10.52202/072781-0085

6. J. S. Weaver, S. R. Kalidindi, *Mechanical characterization of Ti-6Al-4V titanium alloy at multiple length scales using spherical indentation stress-strain measurements*, Materials & Design, 111, **2016** 463 https://doi.org/10.1016/j.matdes.2016.09.016.

7. C. Chang, M. A. Garrido, J. Ruiz-Hervias, Z. Zhang, L. L. Zhang, *Representative Stress-Strain Curve by Spherical Indentation on Elastic-Plastic Materials*, Adv. Mater. Sci. Eng., **2018** 8316384 https://doi.org/10.1155/2018/8316384.

8. F. Pohl, *A Methodology for Inverse Determination of Stress-strain Curves Based on Spherical Indentation*, Experimental Techniques, 42, **2018** 343 https://doi.org/10.1007/s40799-018-0238-1.

9. T. R. Zhang, S. Wang, W. Q. Wang, *Method to determine the optimal constitutive model from spherical indentation tests*, Results in Physics, 8, **2018** 716 https://doi.org/10.1016/j.rinp.2018.01.019.

10. H. Chen, L. X. Cai, C. Bao, *A novel model for determining tensile properties and hardness of steels by spherical indentations*, Strain, 56, **2020** 14 https://doi.org/10.1111/str.12365.

11. A. R. H. Midawi, N. Huda, C. H. M. Simha, A. P. Gerlich, *Characterization of Anisotropy of Strength in API-X80 Line Pipe Welds Through Instrumented Indentation*, Metallography Microstructure and Analysis, 9, **2020** 884 https://doi.org/10.1007/s13632-020-00693-8.

12. K. Goto, I. Watanabe, T. Ohmura, *Inverse estimation approach for elastoplastic properties using the load-displacement curve and pile-up topography of a single Berkovich indentation*, Materials & Design, 194, **2020** 8 https://doi.org/10.1016/j.matdes.2020.108925.

13. F. Y. Huang, Y. W. Liu, J. C. Kuo, *Uncertainties in the representative indentation stress and strain using spherical nanoindentation*, Applied Nanoscience, **2021** 15 https://doi.org/10.1007/s13204-020-01646-x.

14. S. Mohan, N. Millan-Espitia, M. Yao, N. V. Steenberge, S. R. Kalidindi, *Critical Evaluation of Spherical Indentation Stress-Strain Protocols for the Estimation of the Yield Strengths of Steels*, Experimental Mechanics, 61, **2021** 641 https://doi.org/10.1007/s11340-021-00689-7.

15. A. H. Mahmoudi, S. H. Nourbakhsh, R. Amali, *An Alternative Approach to Determine Material Characteristics Using Spherical Indentation and Neural Networks for Bulk Metals*, Journal of Testing and Evaluation, 40, **2012** 211 https://doi.org/10.1520/jte103897.

16. K. Jeong, H. Lee, O. M. Kwon, J. Jung, D. Kwon, H. N. Han, *Prediction of uniaxial tensile flow using finite element-based indentation and optimized artificial neural networks*, Materials & Design, 196, **2020** Art. 109104 https://doi.org/10.1016/j.matdes.2020.109104.

17. L. Lu, M. Dao, P. Kumar, U. Ramamurty, G. E. Karniadakis, S. Suresh, *Extraction of mechanical properties of materials through deep learning from instrumented indentation*, Proc. Nat. Acad. Sci. USA, 117, **2020** 7052 https://doi.org/10.1073/pnas.1922210117.

18. J. E. Campbell, H. Zhang, M. Burley, M. Gee, A. T. Fry, J. Dean, T. W. Clyne, *A Critical Appraisal of the Instrumented Indentation Technique (IIT) and Profilometry-based Inverse FEM Indentation Plastometry (PIP) for Obtaining Stress-Strain Curves*, Adv. Eng. Mats., 23, **2021** 2001496 https://doi.org/10.1002/adem.202001496.

19. C. Heinrich, A. M. Waas, A. S. Wineman, *Determination of material properties using nanoindentation and multiple indenter tips*, Int. J. Solids and Structures, 46, **2009** 364 https://doi.org/10.1016/j.ijsolstr.2008.08.042.

20. J. Dean, J. M. Wheeler, T. W. Clyne, *Use of Quasi-Static Nanoindentation Data to Obtain Stress-Strain Characteristics for Metallic Materials*, Acta Materialia, 58, **2010** 3613 https://doi.org/10.1016/j.actamat.2010.02.031.

21. D. K. Patel, S. R. Kalidindi, *Correlation of spherical nanoindentation stress-strain curves to simple compression stress-strain curves for elastic-plastic isotropic materials using finite element models*, Acta Materialia, 112, **2016** 295 https://doi.org/10.1016/j.actamat.2016.04.034.

22. J. Dean, T. W. Clyne, *Extraction of Plasticity Parameters from a Single Test using a Spherical Indenter and FEM Modelling*, Mechanics of Materials, 105, **2017** 112 https://doi.org/10.1016/j.mechmat.2016.11.014.

23. J. E. Campbell, R. P. Thompson, J. Dean, T. W. Clyne, *Experimental and Computational Issues for Automated Extraction of Plasticity Parameters from Spherical Indentation*, Mechanics of Materials, 124, **2018** 118 https://doi.org/10.1016/j.mechmat.2018.06.004.

24. L. Meng, P. Breitkopf, B. Raghavan, G. Mauvoisin, O. Bartier, X. Hernot, *On the study of mystical materials identified by indentation on power law and Voce hardening solids*, Int. J. Mat. Forming, 12, **2019** 587 https://doi.org/10.1007/s12289-018-1436-1.

25. H. Xue, J. X. He, W. N. Jia, J. L. Zhang, S. Wang, S. Zhang, H. L. Yang, Z. Wang, *An approach for obtaining mechanical property of austenitic stainless steel by using continuous indentation test analysis*, Structures, 28, **2020** 2752 https://doi.org/10.1016/j.istruc.2020.11.001.

26. J. Lee, C. Lee, B. Kim, *Reverse analysis of nano-indentation using different representative strains and residual indentation profiles*, Materials & Design, 30, **2009** 3395 https://doi.org/10.1016/j.matdes.2009.03.030.

27. W. Z. Yao, C. E. Krill, B. Albinski, H. C. Schneider, J. H. You, *Plastic material parameters and plastic anisotropy of tungsten single crystal: a spherical micro-indentation study*, Journal of Materials Science, 49, **2014** 3705 https://doi.org/10.1007/s10853-014-8080-z.

28. M. Z. Wang, J. J. Wu, Y. Hui, Z. K. Zhang, X. P. Zhan, R. C. Guo, *Identification of elastic-plastic properties of metal materials by using the residual imprint of spherical indentation*, Mat. Sci. & Eng. A, 679, **2017** 143 https://doi.org/10.1016/j.msea.2016.10.025.

29. J. E. Campbell, R. P. Thompson, J. Dean, T. W. Clyne, *Comparison between stress-strain plots obtained from indentation plastometry, based on residual indent profiles, and from uniaxial testing*, Acta Materialia, 168, **2019** 87 https://doi.org/10.1016/j.actamat.2019.02.006.

30. P. Hausild, A. Materna, J. Nohava, *On the identification of stress-strain relation by instrumented indentation with spherical indenter*, Materials & Design, 37, **2012** 373 https://doi.org/10.1016/j.matdes.2012.01.025.

31. G. Pintaude, A. R. Hoechele, *Experimental analysis of indentation morphologies after spherical indentation*, Materials Research, 17, **2014** 56 https://doi.org/10.1590/S1516-14392013005000154.

32. T. W. Clyne, J. E. Campbell, *Testing of the Plastic Deformation of Metals*. 2021, Cambridge, U.K.: Cambridge University Press. https://doi.org/10.1017/9781108943369.

33. E. C. Teague, F. E. Scire, S. M. Baker, S. W. Jensen, *3-Dimensional Stylus Profilometry*, Wear, 83, **1982** 1 https://doi.org/10.1016/0043-1648(82)90335-0.

34. A. G. Marrugo, F. Gao, S. Zhang, *State-of-the-art active optical techniques for three-dimensional surface metrology: a review Invited*, J. Opt. Soc. America - A, 37, **2020** B60 https://doi.org/10.1364/josaa.398644.

35. J. H. Hollomon, *Tensile Deformation*, Trans. Amer. Inst. Min. & Metall. Eng., 162, **1945** 268

36. E. Voce, *The Relationship between Stress and Strain for Homogeneous Deformation*, J. Inst. Metals, 74, **1948** 537

37. T. Belytschko, R. Gracie, G. Ventura, *A review of extended/generalized finite element methods for material modeling*, Modelling & Simulation in Mat. Sci. & Eng., 17, **2009** 043001 https://doi.org/10.1088/0965-0393/17/4/043001.

38. F. Roters, P. Eisenlohr, L. Hantcherli, D. D. Tjahjanto, T. R. Bieler, D. Raabe, *Overview of constitutive laws, kinematics, homogenization and multiscale methods in crystal plasticity finite-element modeling: Theory, experiments, applications*, Acta Materialia, 58, **2010** 1152 https://doi.org/10.1016/j.actamat.2009.10.058.

 https://doi.org/10.52202/072781-0085

39. H. Ghaednia, S. A. Pope, R. L. Jackson, D. B. Marghitu, *A comprehensive study of the elasto-plastic contact of a sphere and a flat*, Tribology International, 93, **2016** 78 https://doi.org/10.1016/j.triboint.2015.09.005.

40. A. E. Giannakopoulos, S. Suresh, *Determination of elastoplastic properties by instrumented sharp indentation*, Scripta Materialia, 40, **1999** 1191 https://doi.org/10.1016/s1359-6462(99)00011-1.

41. B. Taljat, G. M. Pharr, *Development of pile-up during spherical indentation of elastic-plastic solids*, Int. J. Sol. Struct., 41, **2004** 3891 https://doi.org/10.1016/j.ijsolstr.2004.02.033.

42. V. Karthik, P. Visweswaran, A. Bhushan, D. N. Pawaskar, K. V. Kasiviswanathan, T. Jayakumar, B. Raj, *Finite element analysis of spherical indentation to study pile-up/sink-in phenomena in steels and experimental validation*, Int. J. Mech. Sci., 54, **2012** 74 https://doi.org/10.1016/j.ijmecsci.2011.09.009.

43. M. Fardi, R. Abraham, P. D. Hodgson, S. Khoddam, *A New Horizon for Barreling Compression Test: Exponential Profile Modeling*, Adv. Eng. Mats., 19, **2017** 1700328 https://doi.org/10.1002/adem.201700328.

44. M. Bol, R. Kruse, A. E. Ehret, *On a staggered iFEM approach to account for friction in compression testing of soft materials*, J. Mech. Behav. Biomedical Mats., 27, **2013** 204 https://doi.org/10.1016/j.jmbbm.2013.04.009.

45. G. Torrente, *Numerical and Experimental Studies of Compression-Tested Copper: Proposal for a New Friction Correction*, Materials Research-Ibero-American J. Materials, 21, **2018** e20170905 https://doi.org/10.1590/1980-5373-mr-2017-0905.

46. X. G. Fan, Y. D. Dong, H. Yang, P. F. Gao, M. Zhan, *Friction assessment in uniaxial compression test: A new evaluation method based on local bulge profile*, J. Materials Processing Techn., 243, **2017** 282 https://doi.org/10.1016/j.jmatprotec.2016.12.023.

47. D. Duran, C. Karadogan, *Determination of Coulomb's Friction Coefficient Directly from Cylinder Compression Tests*, Strojniski Vestnik- J. Mech. Eng., 62, **2016** 243 https://doi.org/10.5545/sv-jme.2015.3141.

48. S. Bellemare, R. Lacy, I. R. Haque, B. Willey. *Addressing the GTI report on HSD process with conclusive evidence*. 2023; Available from: https://bymmt.com/wp-content/uploads/2023/06/mmt_gti_white-paper_v6.pdf.

49. S. Palkovic, P. Patel, S. Safari, S. Bellemare. *A statistical approach to material verification of expected grade through opportunistic field measurements*. in *Pipeline Pigging and Integrity Management (32nd PPIM)*. 2020. Houston.

50. I. R. Haque, B. Feigel, B. Willey, P. Patel, S. Bellemare. *Combining nondestructive techniques to obtain full vintage pipeline asset fracture toughness*. in *Pipeline Pigging and Integrity Management (35th PPIM)*. 2023. Houston.

51. J. Kornuta, J. Anderson, E. Brady, J. Maragh, P. Veloo. *Validating and quantifying in situ NDT uncertainty of line pipe material properties*. in *Pipeline Pigging and Integrity Management (35th PPIM)*. 2023. Houston.

52. J. Anderson, J. Gibbs, O. Oneal, J. A. Kornuta, N. Switzner, P. Veloo. *Using Monte Carlo Simulations to Incorporate Measurement Uncertainty into Grade Predictions*. in *34th International Pipeline Pigging and Integrity Management Conference (PPIM)*. 2022. Houston.

53. J. Anderson, N. Switzner, J. Kornuta, P. Veloo. *Incorporating measurement uncertainty into machine learning-based grade predictions*. in *Proceedings of the 2022 14th International Pipeline Conference (IPC)*. 2022. Calgary.

54. M. Vaisys, *Frictional Sliding in Pipeline Integrity*. 2023.